Supporting information

Efficient Red Thermally Activated Delayed Fluorescence Emitter Achieved Through Precise Control of Excited State Energy Levels.

Bohua Zhang,[a] *Siqi Liu,*[a] *Jiangxue Pei,*[a] *Meiting Luo,*[a] *Yi Chen,*[a] *Qingyu Jia,*[a] Zhaoxin Wu[b] *and Dongdong Wang**[a]

[a] School of Chemistry, Xi'an Jiaotong University, Xi'an 710049, P. R. China.

[b] Key Laboratory for Physical Electronics and Devices of the Ministry of Education & Shaanxi Key Lab of Information Photonic Tech-nique, School of Electronic and Information Engineering, Xi'an Jiaotong University, Xi'an 710049, P. R. China.

Corresponding author: Dongdong Wang

E-mail: ddwang@mail.xjtu.edu.cn

Contents

1. General information

All chemicals and materials, unless otherwise noted, were commercially available and used without further purification. All solvents for reactions and photophysical measurements were of HPLC grade. TGA-DSC measurements from room temperature to 500 °C were carried out on a Shimadzu DTG-60 instrument under dry nitrogen flow with a heating rate of 10 °C/min. Cyclic voltammograms (CV) recorded on a Princeton Applied Research model 273 A electrochemical workstation at a scan rate of 100 mV s^{-1} using 0.1 M tetrabutylammonium perfluorinated phosphorate ($TBAPF_6$) as supporting electrolyte in dry CH_2Cl_2, with a conventional three-electrode system consisting of a glassy carbon working electrode, a platinum wire auxiliary electrode, and an Ag/AgCl standard electrode which was used as the reference electrode. UV-vis absorption spectra of solution were recorded on Hitchi 3010 spectrometers. The steady state and transient fluorescence spectra were measured on FLS 980 fluorescent spectrometer, and PLQY was measured via using the integrating sphere in combination with FLS980 spectrofluorometer.

2. Device fabrication and characterization

All the organic layers were successively deposited by means of vacuum deposition onto the ITO-coated glass substrates, which were previously etched, patterned, and washed with detergent, deionized water, acetone, and ethanol in turn. For the doped layer, the dopant and host materials were co-evaporated and the doping concentrations was controlled by deposition rates. The electroluminescence (EL) spectra and CIE coordinates of the devices were measured by a spectrometer (PR650) and the current-voltage-luminescence characteristics were analyzed using Keithley 2400 source meter with PR650.

3. Computational details

All calculations were performed using the Gaussian 09 program package.[1] The ground state geometries were optimized via DFT calculations at the PBE0-1/3 and 6-31G* level in vacuum. Frequency analysis was used to confirm that the structures are

at the global minimum point of the potential surfaces. Based on the optimized ground state, the lowest excited singlet state (S_1) and lowest triplet states (T_1) configurations are optimized using the TD-DFT method at the PBE0-1/3 and 6-31G* level. Furthermore, the implicit polarizable continuum model (PCM)[2] is used to consider the solvent effects of toluene. Spin–orbit coupling matrix elements (SOCMEs) are gained using the TD-PBE0/TZVP[3] method with the zero-order regular approximation (ZORA)[4] as implemented in the ORCA 4.2.1 program.[5]

4. Synthesis

All solvents and reagents were purchased from commercial sources and used as received without futher purification.The synthetic routes of the targe compounds are outlined as below.

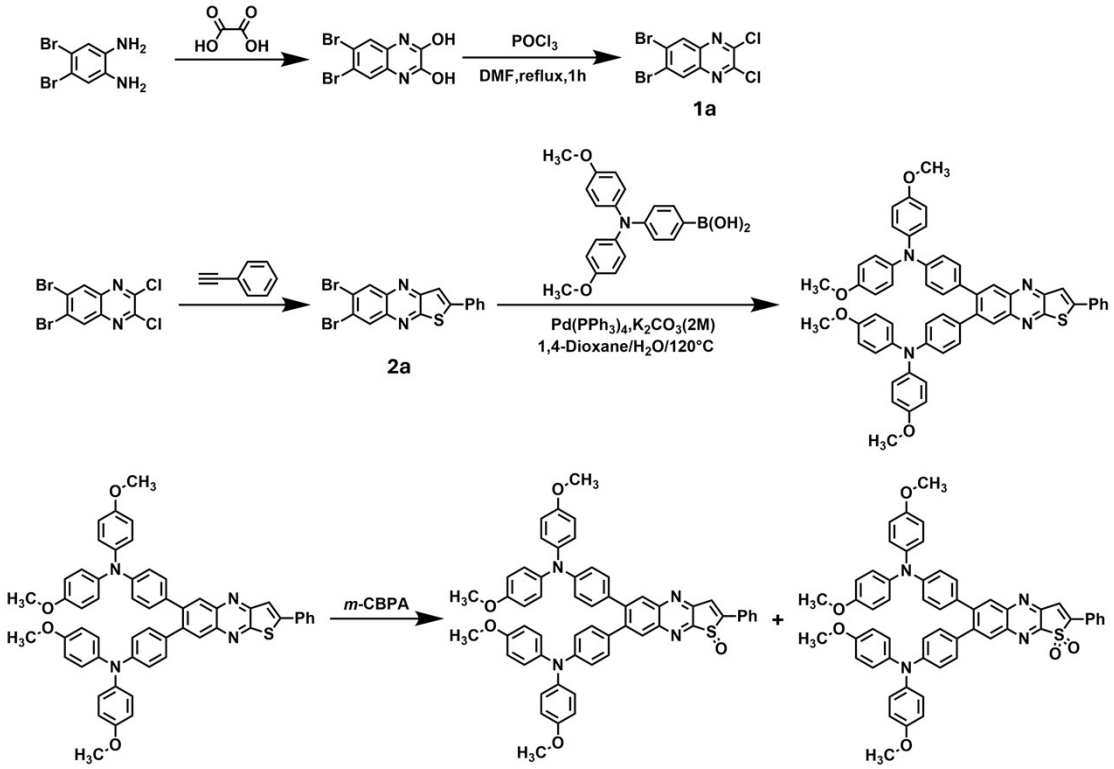

Scheme S1. The synthetic routes of the targe compounds.

Synthesis of 2,3-dichloro-6,7-dibromoquinoxaline (intermediate 1a):

In a dry flask, add 4,5-dibromo-o-phenylenediamine (1.0 g, 3.76 mmol), oxalic acid (0.52 g, 4.14 mmol), 200-300 mesh silica gel powder (3 g), toluene (20 mL), displace the air with nitrogen, and react at 110℃ for 5 hours. After the thin layer chromatography plate (TLC) detects the completion of the reaction, do not treat the reaction and directly slowly add $POCl_3$ (8.4 mL) and DMF (5 mL) to the system, and continue to react at 110℃ for 1 hour. After the TLC detects the completion of the reaction, add 100 mL of ice water for quenching, then add 100 mL of ethyl acetate for extraction. After several extractions, combine the organic layers, dry with anhydrous sodium sulfate, and evaporate the solvent to obtain 1.2 g of white solid with a yield of 89%. ^{1}H NMR (400MHz, DMSO-d6) δ(ppm): 8.20(s, 2H).

Synthesis of *6,7-dibromo-2-phenylthieno[2,3-b]quinoxaline* (intermediate 2a):

2,3-dichloro-6,7-dibromoquinoxalin (0.6 g, 1.68 mmol) was dissolved in MeCN (20 mL), then Pd $(PPh_3)_2Cl_2$ (5 mol-%) and CuI (5 mol-%) were added. The reaction flask was then sealed and flushed with nitrogen. Then, Et_3N (2.5 equiv.) and ethynylbenzene (0.18 g, 1.75 mmol) were added. The reaction mixture was stirred at 60 °C for 8 h. After the first coupling reaction was complete, NaSH·xH2O (5.0 equiv.) in dimethylformamide (2 mL) was added. The reaction mixture was then was refluxed until TLC revealed complete conversion of the intermediate into the final product. The mixture was then cooled, diluted with H_2O and filtered. The residue was purified by silica gel column chromatography (CH_2Cl_2/petroleum ether) to give the corresponding product 2a (0.6g, 88%). ^{1}H NMR (400 MHz, Chloroform-d) δ 8.55 (s, 1H), 8.48 (s, 1H), 7.88 -7.84 (m, 2H), 7.82 (s, 1H), 7.54 (t, 3H).

Synthesis of TQ-oMeOTPA:

6,7-dibromo-2-phenylthieno[2,3-b]quinoxaline (0.84 g, 2.0 mmol), (4-(bis(4-methoxyphenyl)amino)phenyl)boronic acid (2.11 g, 6.0 mmol), K_2CO_3 (1.67 g, 12.8 mmol) and Pd$(PPh_3)_4$ (0.23 g, 0.2 mmol) were added to 150 ml dioxane/H2O (4:1) mixed solvent. Then the reaction mixture was stirred at 120°C under a nitrogen

atmosphere until TLC revealed complete conversion of the starting material. The mixture was cooled, diluted with H_2O and filtered. The residue was purified by silica gel column chromatography (CH_2Cl_2/petroleum ether) to give expected product TQ-oMeOTPA (1.42 g, 83%). ^{1}H NMR (600 MHz, DMSO-d6) δ 8.23 (s, 1H), 8.07-8.01 (m, 4H), 7.61-7.54 (m, 3H), 7.09-7.05 (m, 12H), 6.9 (d, J = 8.6 Hz, 8H), 6.73 - 6.71 (m, 4H), 3.75 (s, 12H). ^{13}C NMR (150 MHz, $CDCl_3$) δ 156.68, 156.13, 143.37, 143.19, 140.82, 139.82, 133.41, 130.69, 130.53, 129.45, 129.08, 128.72, 127.00, 126.92, 119.69, 117.15, 114.84, 58.61, 55.63. HRMS(ESI) calculated for $C_{56}H_{44}N_4O_4S$ $[M+H]^+$ 869.3156, found: 869.3122.

Synthesis of TsQ-oMeOTPA and SQ-oMeOTPA:

To a mixture of an appropriate compound **TQ-oMeOTPA** (0.5 mmol) in DCM (50 mL) in a round-bottom flask at 0°C, m-CPBA (0.6 mmol) was added and the resulting mixture stirred for 24h, monitored by TLC and then concentrated under reduced pressure and purified by column chromatography using petroleum CH_2Cl_2/petroleum ether to afford the corresponding products (**TsQ-oMeOTPA, SQ-oMeOTPA**) in low yield (23% and 15% respectively).

TsQ-oMeOTPA:^{1}H NMR (400 MHz, DMSO-d6) δ 8.39 (s, 1H), 8.28 (s, 1H), 8.06 (s, 1H), 8.03 -7.97 (m, 2H), 7.61 - 7.50 (m, 3H), 7.09-7.05 (m, 12H), 6.95 - 6.89 (m, 8H), 6.73-6.70 (m, 4H), 3.75 (s, 12H). ^{13}C NMR (150 MHz, $CDCl_3$) δ 157.72, 148.53, 144.35, 142.35, 138.91, 133.68, 132.75, 130.43, 129.40, 129.17, 126.80, 114.58, 110.63, 58.49, 55.49. HRMS(ESI) calculated for $C_{56}H_{44}N_4O_5S$ $[M+H]^+$ 885.3032, found: 885.3056.

SQ-oMeOTPA: ^{1}H NMR (400 MHz, DMSO-d6) δ 8.38 (s, 1H), 8.22 (s, 1H), 8.11 (s, 1H), 8.02-8.00 (m, 2H), 7.59-7.55 (m, 3H), 7.10-7.05 (m, 12H), 6.93-6.91 (m, 8H), 6.73-6.70 (m, 4H), 3.74 (s, 12H). ^{13}C NMR (150 MHz, $CDCl_3$) δ 155.47, 152.03, 150.83, 139.69, 138.49, 137.90, 133.56, 131.42, 130.17, 129.26, 129.06, 128.25, 127.07, 126.80, 125.32, 117.70, 114.71, 58.49, 55.53. HRMS(ESI) calculated for $C_{56}H_{44}N_4O_6S$ $[M+H]^+$ 901.3104, found: 901.3110.

5. Supplemental Figures and Tables

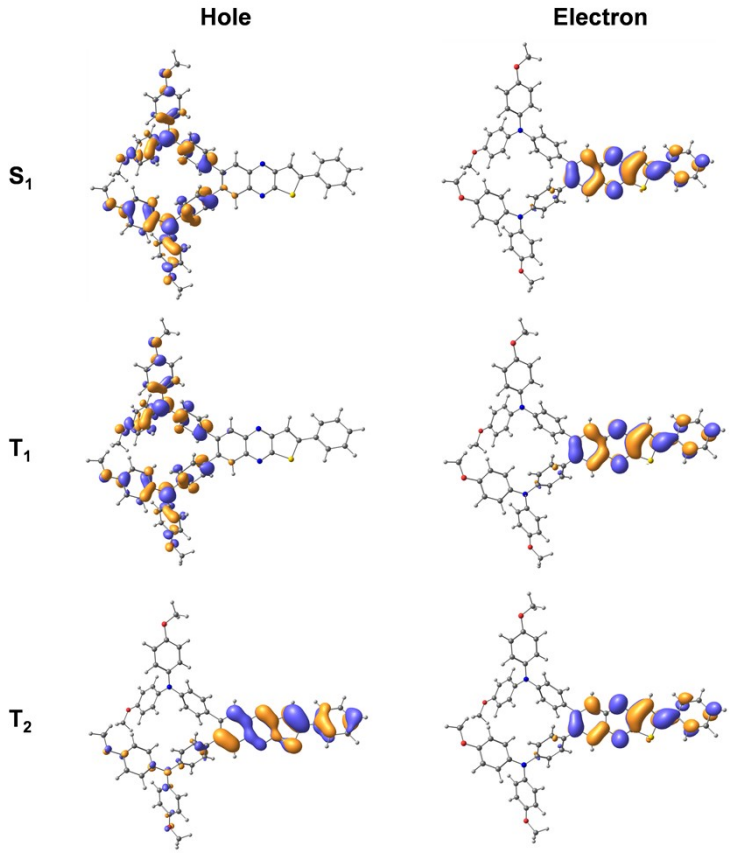

Fig S1. The calculated natural transition orbitals (NTOs) of **TQ-oMeOTPA**

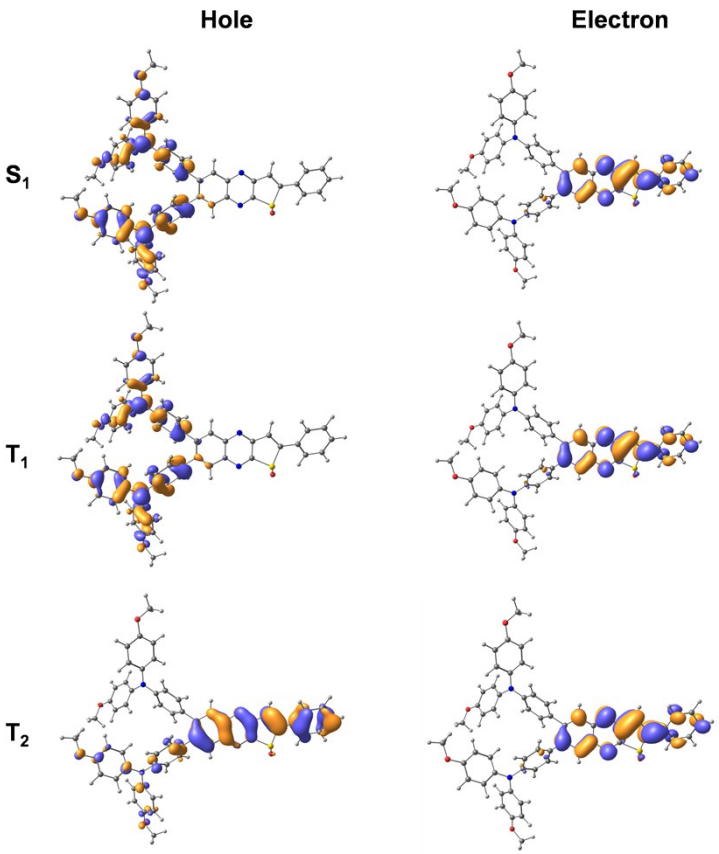

Fig S2. The calculated natural transition orbitals (NTOs) of **TsQ-oMeOTPA**

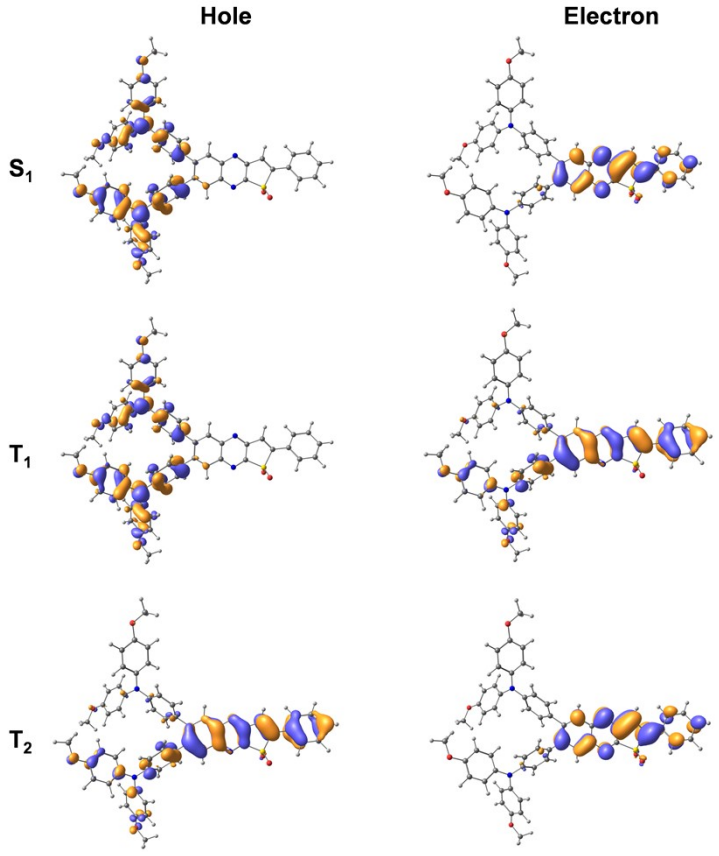

Fig S3. The calculated natural transition orbitals (NTOs) of **SQ-oMeOTPA**

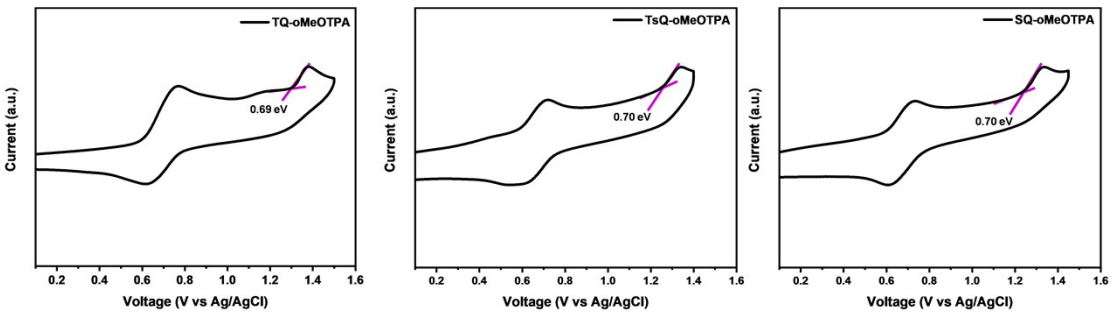

Fig S4. Cyclic voltammetry analysis of **TQ-oMeOTPA**, **TsQ-oMeOTPA** and **SQ-oMeOTPA**.

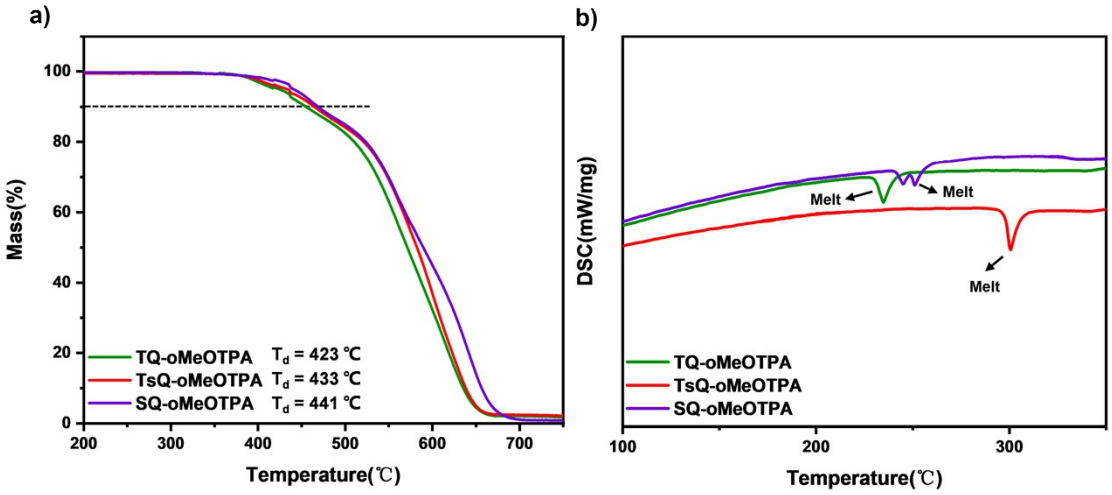

Fig S5. (a) TGA and (b) DSC thermograms of **TQ-oMeOTPA**, **TsQ-oMeOTPA** and **SQ-oMeOTPA**.

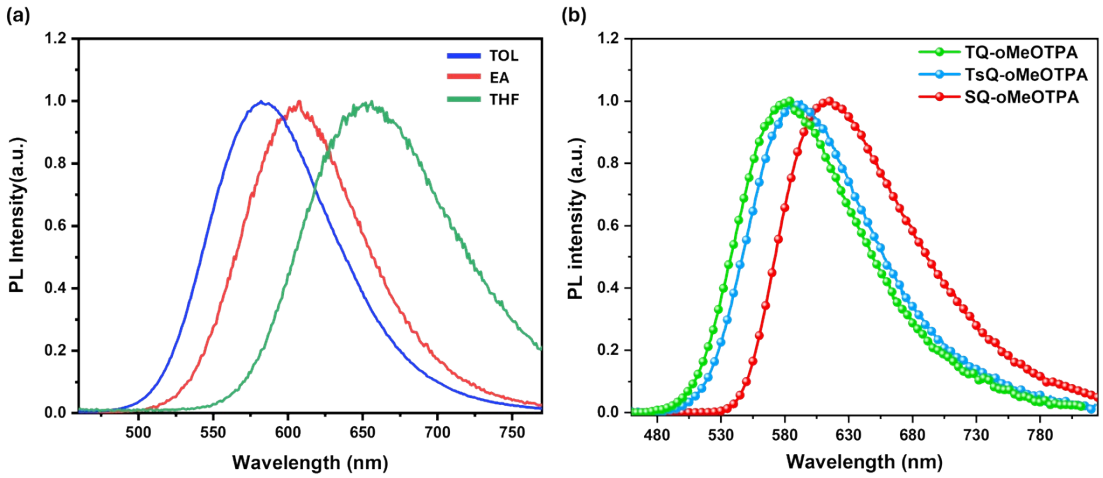

Fig. S6. (a) PL spectra of **TQ-oMeOTPA** in different solvents measured at room temperature. (b) PL spectra of the molecules in doped films (3wt%)

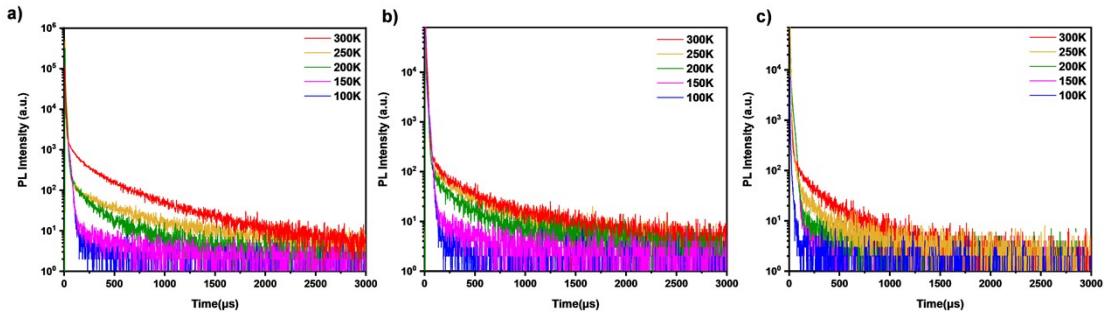

Fig. S7. Transient PL decay curves of 3wt% mCBP doped film at different temperatures. **(a) TQ-oMeOTPA (b) TsQ-oMeOTPA** and **(c) SQ-oMeOTPA**.

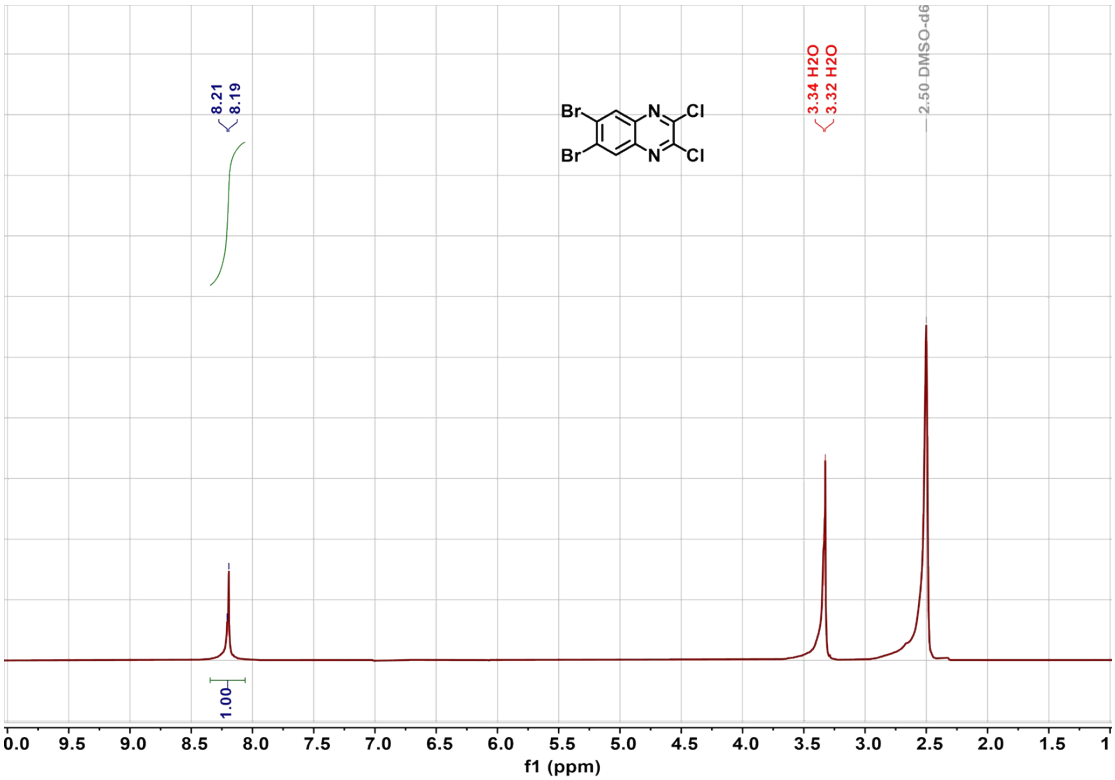

Fig. S8. ^{1}H-NMR spectrum of 2,3-dichloro-6,7-dibromoquinoxaline in deuterated DMSO-d6 solvent.

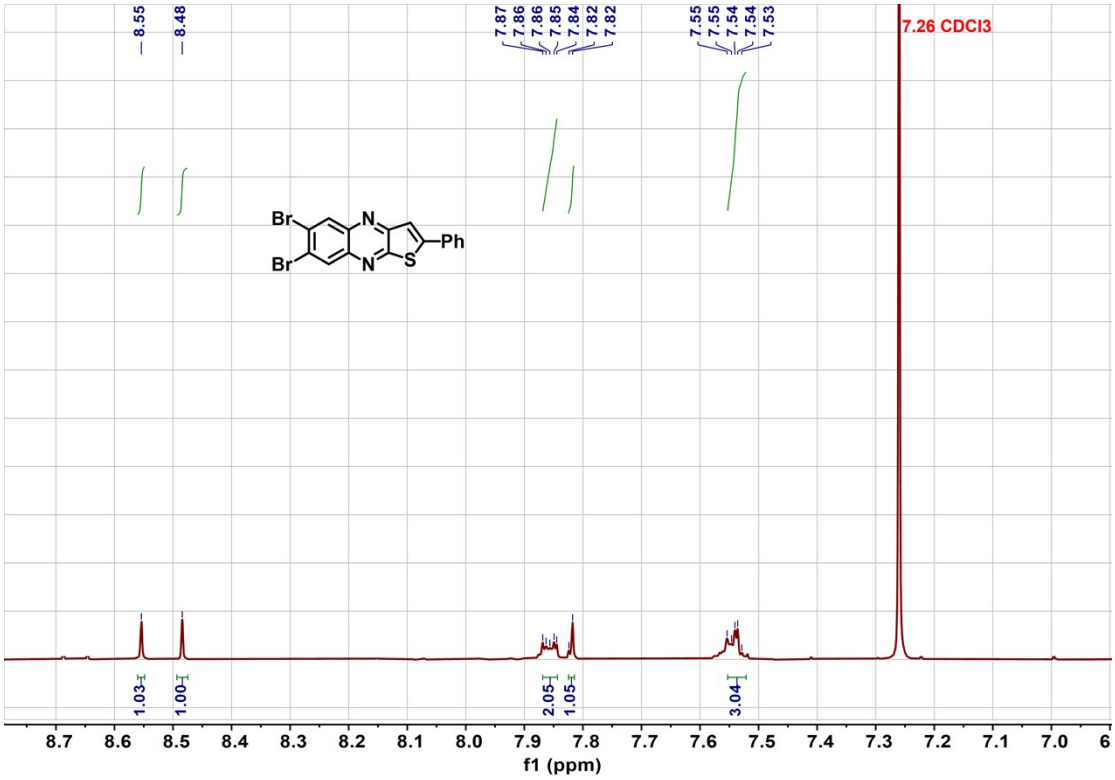

Fig. S9. ^{1}H-NMR spectrum of 6,7-dibromo-2-phenylthieno[2,3-b]quinoxaline in deuterated $CDCl_3$ solvent.

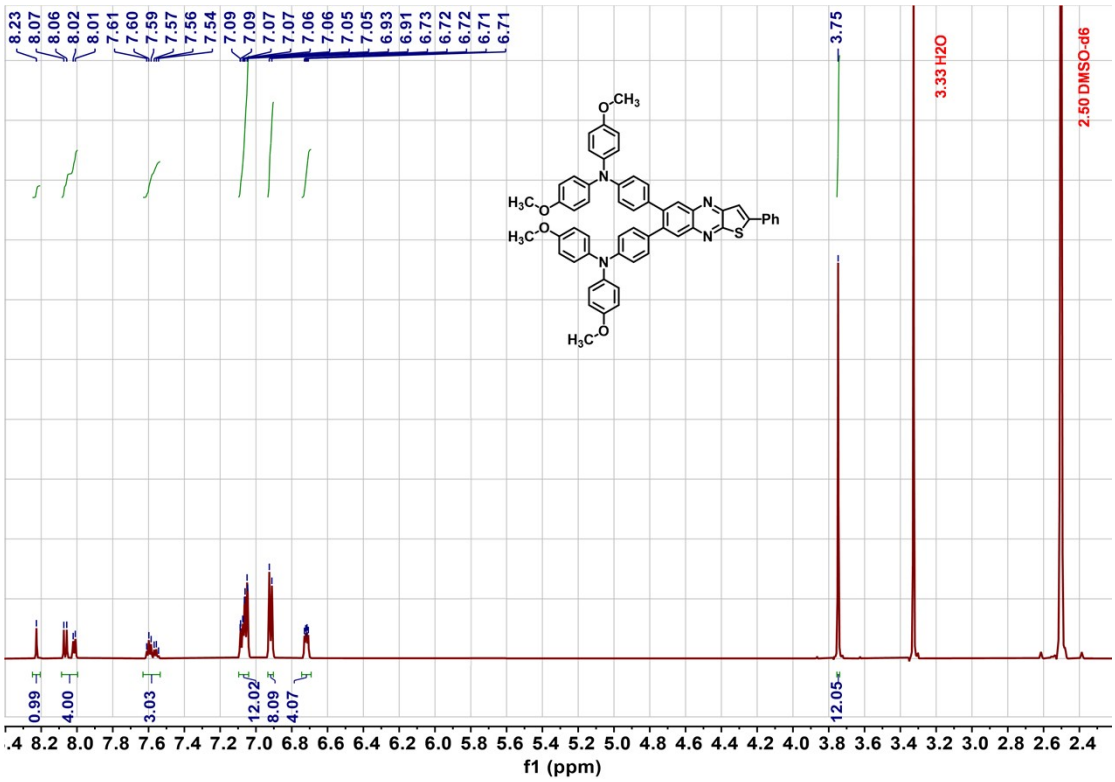

Fig. S10. ^{1}H-NMR spectrum of compound **TQ-oMeOTPA** in deuterated DMSO-d6

solvent.

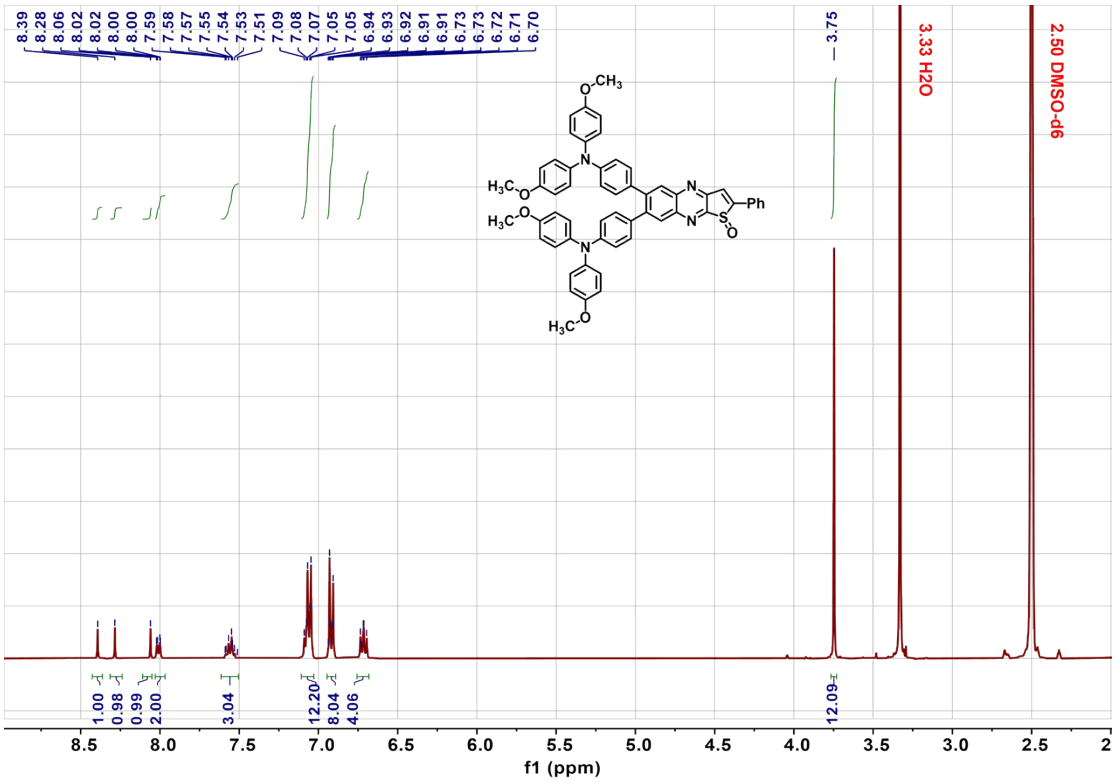

Fig. S11. [1]H-NMR spectrum of compound **TsQ-oMeOTPA** in deuterated DMSO-d6 solvent.

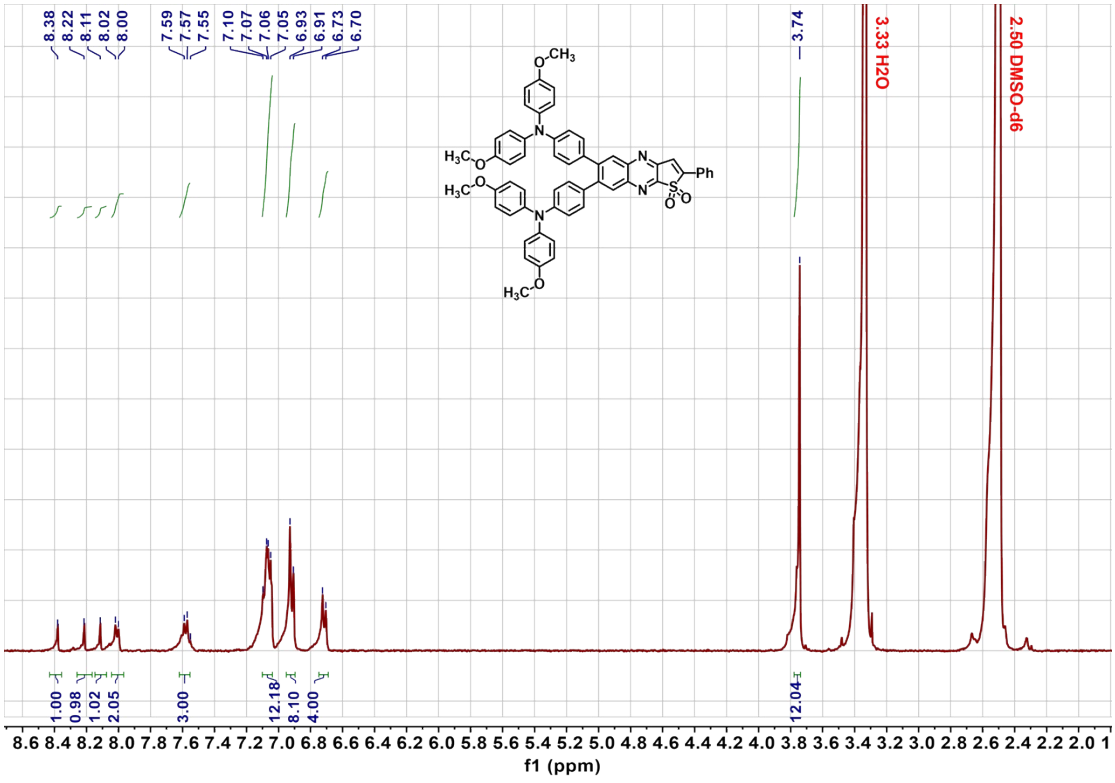

Fig. S12. [1]H-NMR spectrum of compound **SQ-oMeOTPA** in deuterated DMSO-d6

solvent.

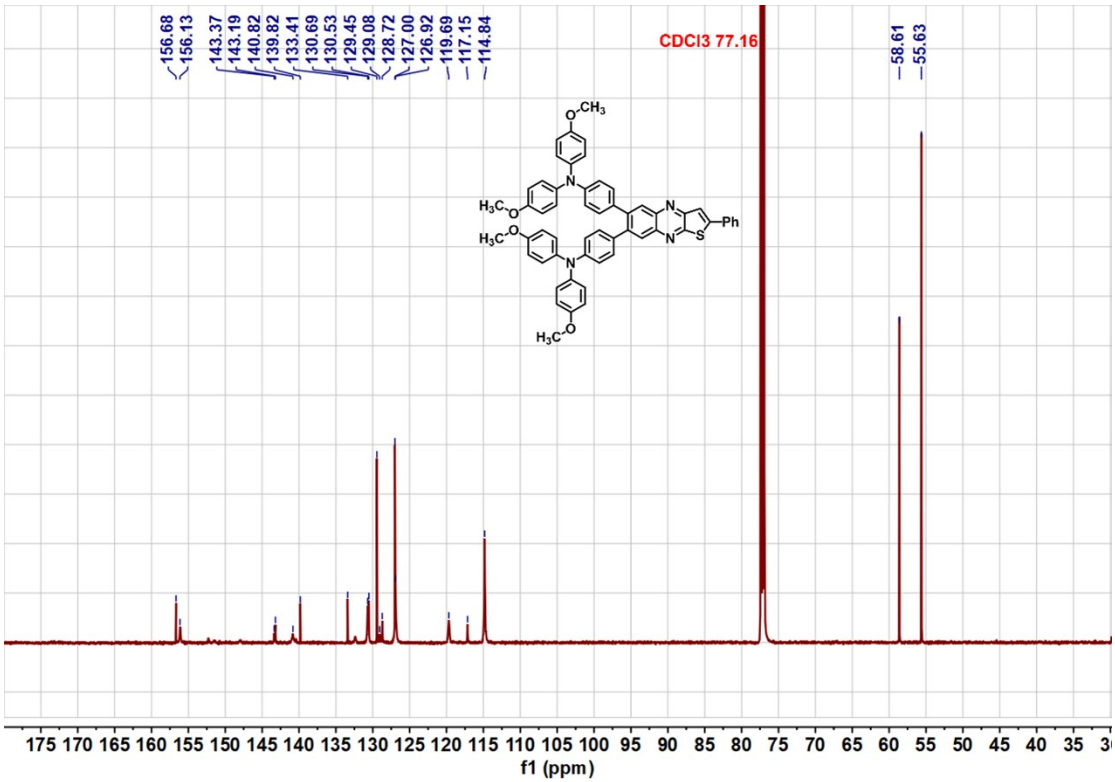

Fig. S13. ^{13}C NMR of compound **TQ-oMeOTPA** in deuterated $CDCl_3$ solvent.

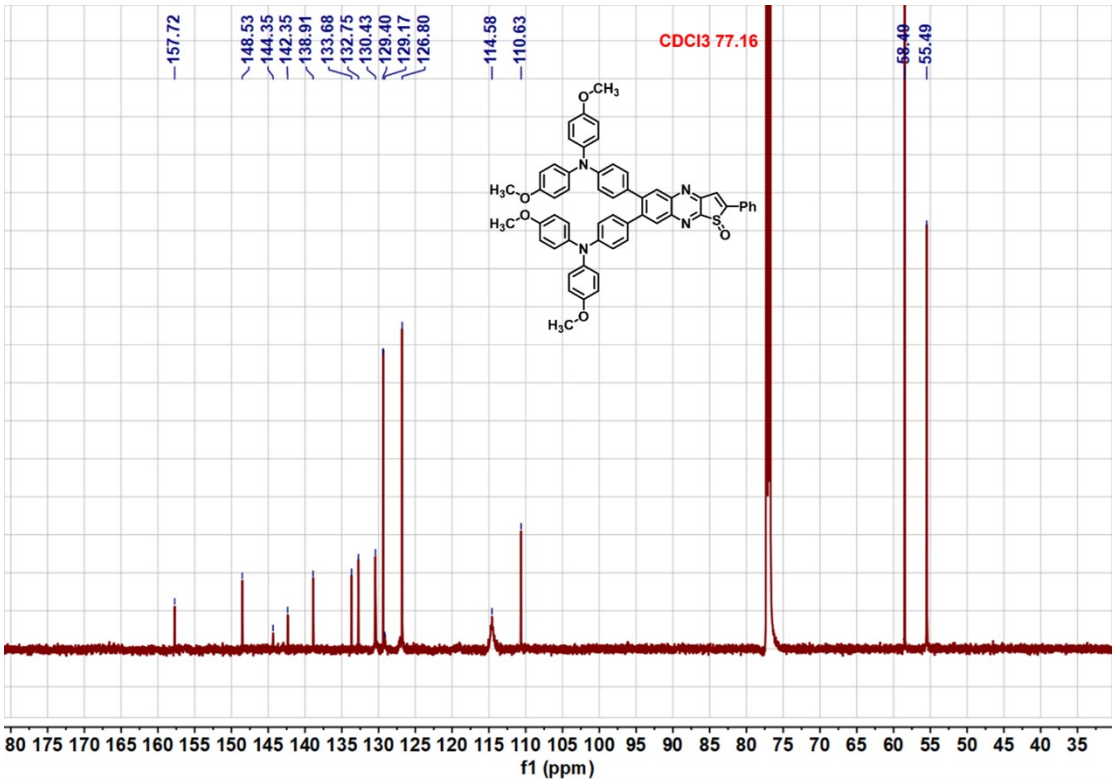

Fig. S14. ^{13}C NMR of compound **TsQ-oMeOTPA** in deuterated $CDCl_3$ solvent.

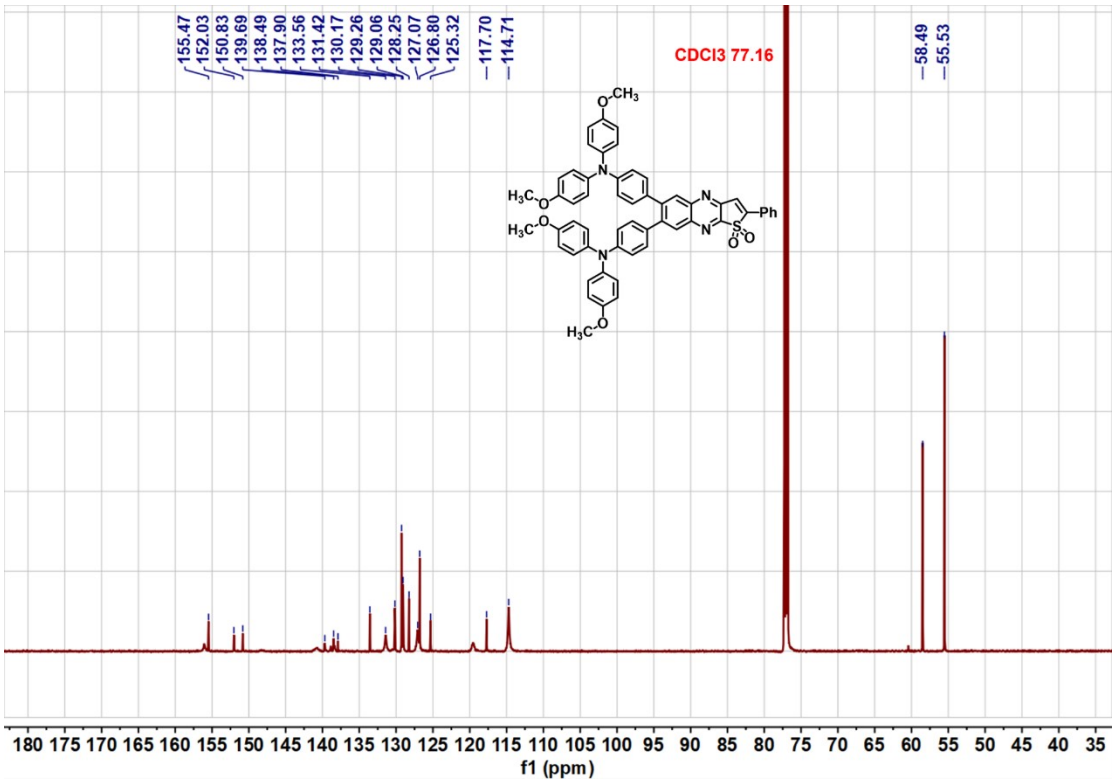

Fig. S15. ^{13}C NMR of compound **SQ-oMeOTPA** in deuterated $CDCl_3$ solvent.

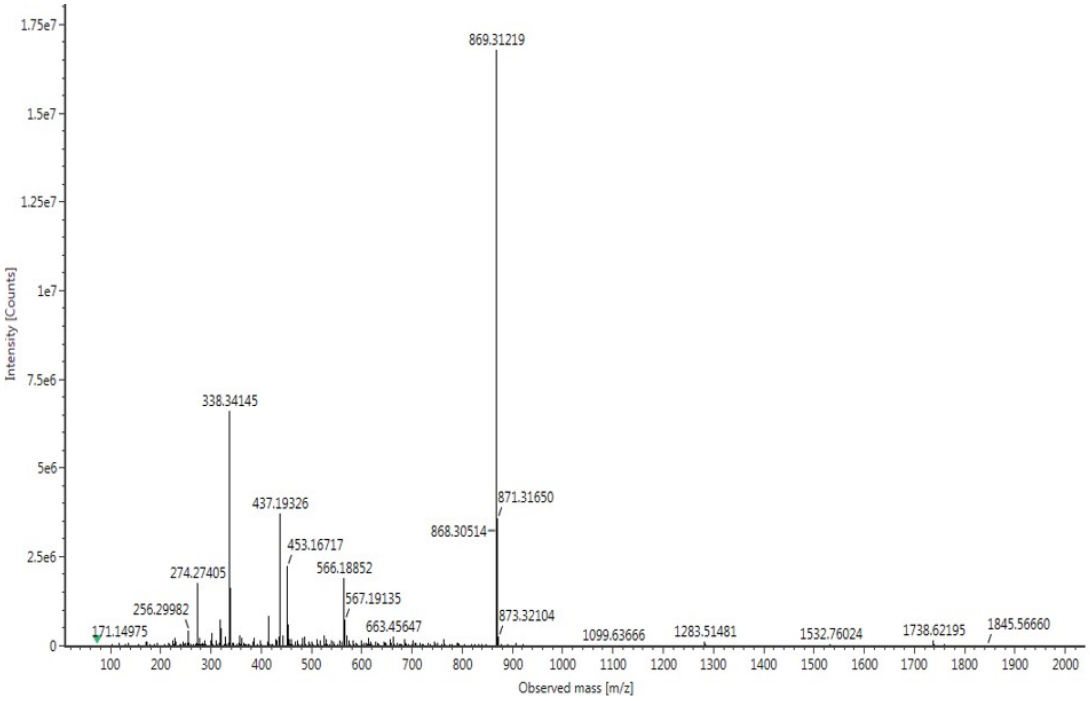

Fig. S16. MS spectrum of **TQ-oMeOTPA**.

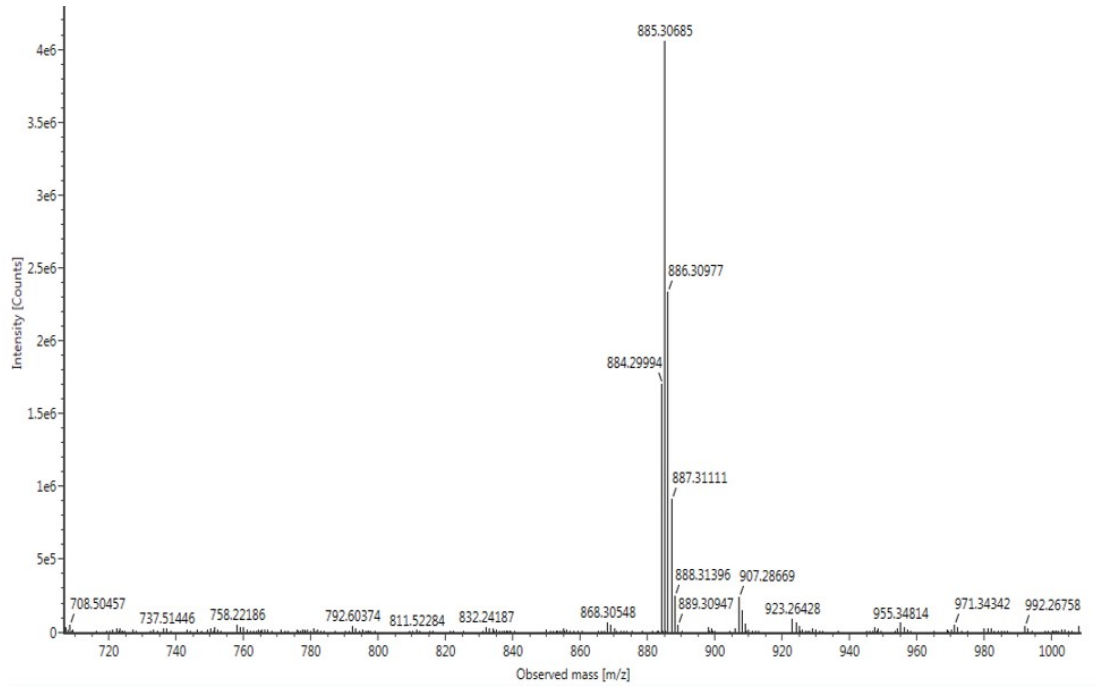

Fig. S17. MS spectrum of **TsQ-oMeOTPA**.

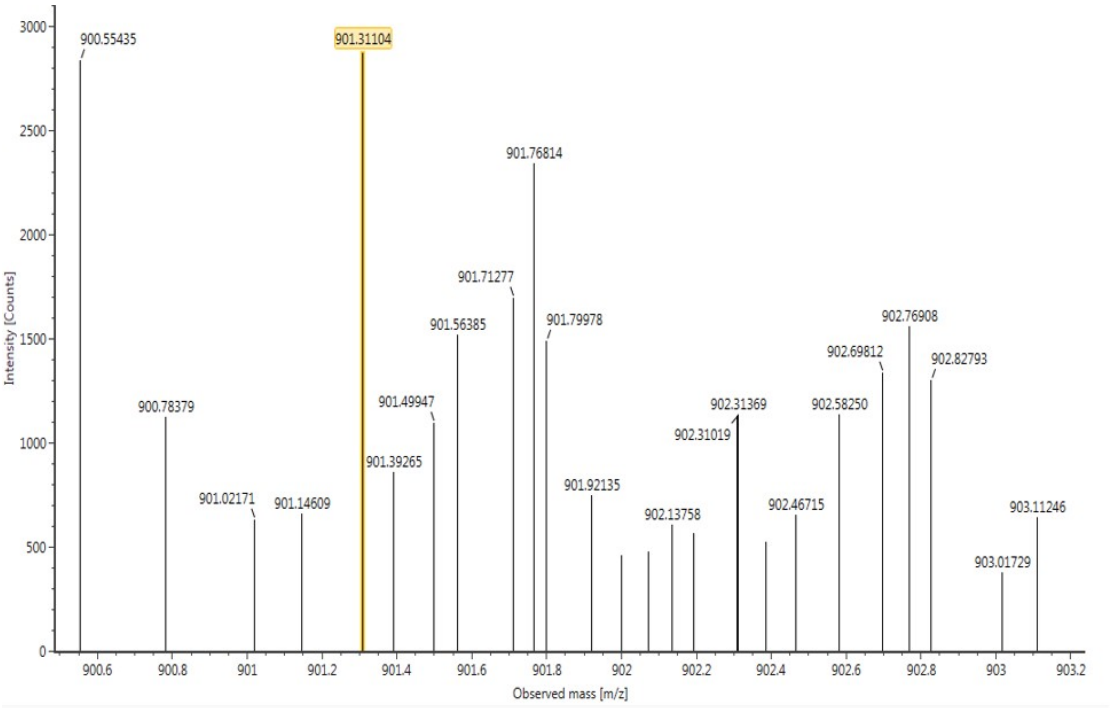

Fig. S18. MS spectrum of **SQ-oMeOTPA**.

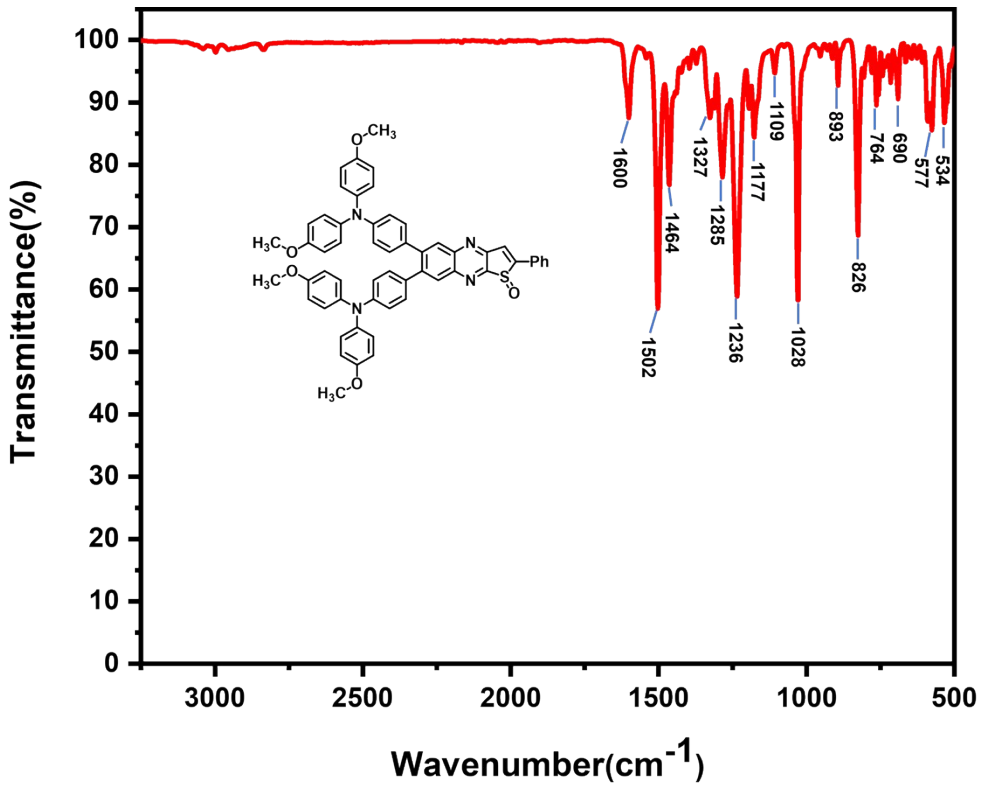

Fig. S19. IR Spectra of **TsQ-oMeOTPA.**

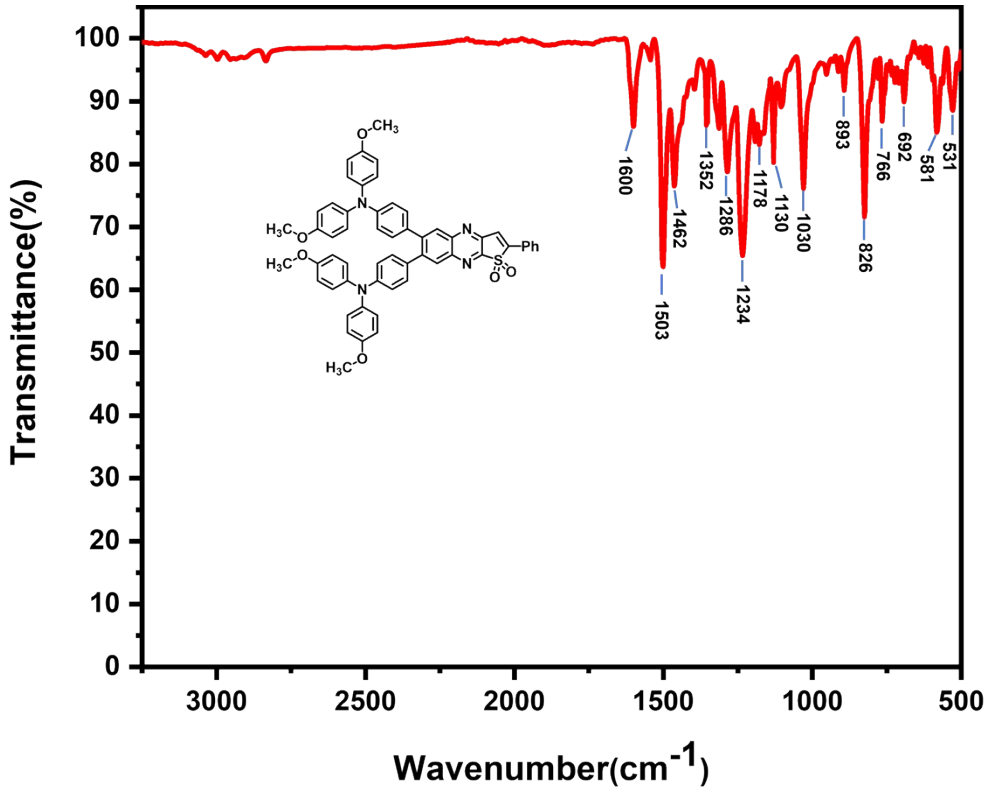

Fig. S20. IR Spectra of **SQ-oMeOTPA.**

Table S1. Summary of the computational data of the molecules

Parameter	Functional	TQ-oMeOTPA	TsQ-oMeOTPA	SQ-oMeOTPA
$E_{VA}(S_1)$ (eV)	BLYP (0%)	1.34	1.22	1.13
	B3LYP (20%)	2.12	2.00	1.89
	PBE0-1/3(33%)	2.63	2.52	2.40
	BMK (42%)	2.89	2.78	2.66
	M062X (56%)	3.21	3.13	3.02
	M06HF (100%)	3.57	3.48	3.50
$E_{VA}(T_1)$ (eV)	BLYP (0%)	1.20	1.14	1.04
	B3LYP (20%)	1.95	1.86	1.76
	PBE0-1/3(33%)	1.88	1.89	1.86
	BMK (42%)	2.28	2.30	2.27
	M062X (56%)	2.49	2.54	2.51
	M06HF (100%)	2.95	2.99	3.00
$E_{0\text{-}0}(^3LE)$ (eV) [a]	M06-HF	2.18	2.21	2.22
CT amount (e)	-	0.83	0.84	0.84
optimal HF% [b]	-	35%	35%	35%
E_{VE} (S_1, OHF) (eV) [c]	-	2.26	2.07	1.90
E_{VA} (S_1, OHF) (eV) [c]	Cal.	2.63	2.52	2.40
	Exp.	2.70	2.58	2.55
$E_{0\text{-}0}(^1CT)$ (eV) [d]	Cal.	2.45	2.30	2.15
	Exp.	2.36	2.25	2.08
$E_{0\text{-}0}(^3CT)$ (eV) [e]	Cal.	2.17	2.13	1.97
	Exp.	2.14	2.13	1.91
ΔE_{st}	Cal.	0.26	0.17	0.18
	Exp.	0.22	0.12	0.17

6. References

1. Gaussian 09, Revision A.02, M. J. Frisch, G. W. Trucks, H. B. Schlegel, G. E. Scuseria, M. A. Robb, J. R. Cheeseman, G. Scalmani, V. Barone, G. A. Petersson, H. Nakatsuji, X. Li, M. Caricato, A. Marenich, J. Bloino, B. G. Janesko, R. Gomperts, B. Mennucci, H. P. Hratchian, J. V. Ortiz, A. F. Izmaylov, J. L. Sonnenberg, D. Williams-Young, F. Ding, F. Lipparini, F. Egidi, J. Goings, B. Peng, A. Petrone, T. Henderson, D. Ranasinghe, V. G. Zakrzewski, J. Gao, N. Rega, G. Zheng, W. Liang, M. Hada, M. Ehara, K. Toyota, R. Fukuda, J. Hasegawa, M. Ishida, T. Nakajima, Y. Honda, O. Kitao, H. Nakai, T. Vreven, K. Throssell, J. A. Montgomery, Jr., J. E. Peralta, F. Ogliaro, M. Bearpark, J. J. Heyd, E. Brothers, K. N. Kudin, V. N. Staroverov, T. Keith, R. Kobayashi, J. Normand, K. Raghavachari, A. Rendell, J. C. Burant, S. S. Iyengar, J. Tomasi, M. Cossi, J. M. Millam, M. Klene, C. Adamo, R. Cammi, J. W. Ochterski, R. L. Martin, K. Morokuma, O. Farkas, J. B. Foresman, and D. J. Fox, Gaussian, Inc., Wallingford CT, 2016.
2. J. Tomasi , B. Mennucci and R. Cammi , Chem. Rev., 2005, 105 , 2999 — 3093.
3. J. Zheng , X. Xu and D. G. Truhlar , Theor. Chem. Acc., 2010, 128 , 295 — 305.
4. J. Yang , Z. Ren , Z. Xie , Y. Liu , C. Wang , Y. Xie , Q. Peng , B. Xu , W. Tian , F. Zhang , Z. Chi , Q. Li and Z. Li , Angew. Chem., Int. Ed., 2017, 56 , 880 —884.
5. F. Neese: Software update: the ORCA program system, version 4.0 (WIREs Comput Mol Sci 2018,8:e1327. doi: 10.1002/wcms.1327.